

Spacing Dependent and Doping Independent Superconductivity in Intercalated 1T Two Dimensional SnSe₂

Hanlin Wu^{1*}, Sheng Li^{1*}, Michael Susner², Sunah Kwon³, Moon Kim³, Timothy Haugan², Bing Lv^{1†}

¹ *Department of Physics, The University of Texas at Dallas, Richardson, TX 75080, USA*

² *Air Force Research Laboratory, Aerospace Systems Directorate, Wright-Patterson AFB, OH 87123, USA*

³ *Department of Materials Science and Engineering, University of Texas at Dallas, Richardson, TX 75080, USA*

The weak van der Waals interlayer interactions in the transition metal dichalcogenide (TMD) materials have created a rich platform to study their exotic electronic properties through chemical doping or physical gating techniques. We reported bulk superconductivity up to 7.6 K through careful manipulation of the charge carrier density and interlayer spacing d in the chemically intercalated two dimensional 1T-SnSe₂ phase. We found, for the first time in the two dimensional SnSe₂, that polar organic molecules cointercalated with the alkali metal Li into the basal layers, thus significantly enhancing the superconducting T_c . We observed that the T_c scales with the basal spacing distance, meanwhile being almost independent of x in Li _{x} (THF) _{y} SnSe₂ system. Our results offers a new general chemical route to study the rich electron correlations and the interplay of charge density wave and unconventional superconductivity in the two dimensional material.

I. INTRODUCTION

Two dimensional layered materials such as transition metal dichalcogenides (TMD) have attracted significant research interests in the past decade due to their fantastic physical properties such as layer-dependent band gap [1-3], topology [4-9], and valley-related transport induced by broken inversion symmetry [10-14]. Great progress has been made in the fundamental and nanoscale device studies of these materials towards their potential applications in electronics, optoelectronics, and spintronics [15-18]. The layered feature of these TMDs permits a variety of guest atoms, molecules or electrons to be intercalated into the van der Waals gap of the host materials. Numerous works have reported on the drastic change to the optical and electrical properties of layered materials when they are subjected to intercalation into the van der Waals gaps with group I or II alkali metal atoms or inorganic molecules [19-25]. Superconductivity has been induced in many of these TMD materials through both chemical doping/intercalation [26-31] and physical gating methods [32-36], with the very recent highlight of gate-induced superconductivity in the topological WTe₂ system [37,38].

Comparatively, much fewer efforts have been made in the study of post-transition metal dichalcogenides, which have different electronic structures from TMDs owing to their lack of d -electron contributions to bands near the Fermi surface [39,40]. Tin-based dichalcogenides, for example, crystallized solely in the two dimensional CdI₂-type 1T phase to date [41], similar as MoS₂, where hexagonal closely packed sandwich

layers are stacked with a periodicity of one layer tin atom and two layers chalcogenide atoms forming tilted SnSe₆ octahedra. The interlayer spaces of ~ 5.785 Å for SnS₂ and 6.137 Å for SnSe₂ that are loosely bonded by van der Waals forces. Compared to MoS₂, the larger interlayer spacing in the Sn dichalcogenide materials will result in a higher possible degree of chemical species intercalations as well as provide a buffer for the large volume change associated with the intercalation processes. In fact, superconductivity has been reported through the intercalation of organic metallocenes with possible charge density wave (CDW) interplay at higher temperatures, another signature for unconventional superconductivity [42-44]. Gating techniques have induced superconductivity at 3.9 K with the in plane upper critical field greatly exceed the Pauli limit [45]. In addition, interface superconductivity is suggested in a SnSe₂/graphite heterostructure through STM study [46,47]. The unexpected large superconducting gap bears a number of similarities to that of cuprates, providing additional strong evidence for unconventional superconductivity. In addition, SnSe₂ and SnS₂, are also widely used for solar cells [48], anode of lithium/sodium ion batteries [49,50], field effect transistors [51] and also photodetector [52].

Herein, we report bulk superconductivity up to 7.6 K in the alkali metal Li-intercalated Li _{x} SnSe₂ and the organic molecule cointercalated Li _{x} M _{y} SnSe₂, where M is tetrahydrofuran (THF) or propylene carbonate (PC). We have systematically investigated the controllability of both carrier density x , organic molecules M, and the interlayer spacing d . While an interesting x -independent superconducting transition temperature is preserved, a significant T_c enhancement of up to 100%, depending on the interlayered spacing, was observed by organic molecule cointercalation. Finally, detailed transport studies

* These authors contributed equally to this work

† To whom correspondence should be addressed: blv@utdallas.edu

suggest the presence of unconventional superconductivity in this cointercalated SnSe₂ system.

II. EXPERIMENTAL

The SnSe₂ crystals was synthesized as follows. the mixture of high purity tin ingot (Alfa Aesar, 99.99%) and selenium pieces (Alfa Aesar, 99.999%), were sealed in a evacuate quartz tube heated to 950 °C in 20 hours for 24 hours, and then slowly cooled down to 650 °C to obtain high purity SnSe₂ precursor. The high quality SnSe₂ single crystals are grown through vertical Bridgeman method using the pre-reacted SnSe₂ powder in the doubled sealed quartz tube container, with growth zone at 950 °C, cooling zone at 500 °C, moving rate at 1.5 mm/h and total growth time of 20 days. The grounded powder of SnSe₂ crystals grown from Bridgeman method was used as starting material for our intercalation studies.

Since the Li-intercalated samples are air sensitive, all the intercalation and co-intercalation process were performed inside purified Ar-atmosphere glovebox with total O₂ and H₂O levels < 0.1 ppm. The *n*-butyllithium (*n*-BuLi) used was 2.6 M (1 M = 1 mol/L) concentration in hexane solution from Alfa Aesar and diluted to 0.02 - 0.2 M. Lithium naphthalene solutions (Li-Naph) with concentration of 0.02 - 0.2 M were prepared by dissolving equimolar amounts of naphthalene and Li metal into THF while magnetic stirring and heating at ~ 70 °C. Organic solvents hexane, THF and PC are vacuum distilled and dried with molecular sieve before usage. We used several different intercalation methods to prepare a variety of samples.

(i) Li_{*x*}SnSe₂ samples were prepared by soaking the parent SnSe₂ powder in various diluted 0.02 - 0.2 M *n*-BuLi solution. The *n*-BuLi contained in the solutions is more than three equivalent of actual doping level of SnSe₂ to avoid the dilution of the *n*-BuLi in the intercalation process. (cf. Figure 1a).

(ii) The cointercalated Li_{*x*}(THF)_{*y*}SnSe₂ were prepared by soaking in various concentration (0.02 - 0.4 M) Li-Naph solution in THF with a typical period for 1 day under magnetic stirring. (cf. Figure 1c).

(iii) Since the Li metal does not reacts with naphthalene nor dissolves in the PC solvent, the direct PC cointercalation using method (ii) is not feasible. Alternatively, the PC cointercalated Li_{*x*}(PC)_{*y*}SnSe₂ were prepared by soaking Li-intercalated sample (by method i) in enough PC solution under magnetic stirring. (cf. Figure 1c).

The chemical composition, i.e Li concentration (*x*) in the products was determined within an accuracy of ±0.01 by inductively coupled plasma mass spectroscopy (ICP-MS) using Agilent Technologies 7900. Thus determined *x* values are used throughout the manuscript.

The powder samples were dried, and cold pressed into pellets under uniaxial stress for the following physical measurements. X-ray diffraction patterns were collected using the Rigaku Smartlab. Electrical resistivity ρ was measured by employing a standard 4-probe method down to 1.8 K in a Quantum Design Physical Property Measurement System (PPMS). The

magnetization was carried out using the Quantum Design Magnetic Property Measurement System (MPMS).

III. RESULTS AND DISCUSSION

Because of its two dimensional layered nature, SnSe₂ thin flakes obtained from grinding the Bridgman-grown crystals have very strong *c*-axis preferred orientation in their X-ray diffraction (XRD) patterns. The strongest (001) peak, therefore, is used to compare and determine the lattice expansion during the intercalation process. In Figure 1 we shown the XRD patterns for both the intercalated samples and the parent compound. The use of different organic solvents can severely impact the intercalation process. The polar organic molecules such as THF and PC, with their stronger reducing power due to the cation-dipole interaction, can cointercalate with the cations, but non-polar solvent molecules such as hexane used in *n*-BuLi reaction are not cointercalated.

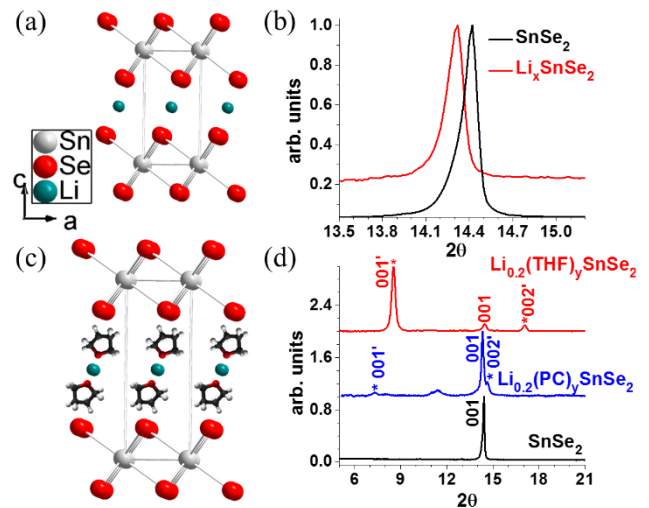


FIG. 1. (a) Schematic structural model for Li-intercalated Li_{*x*}SnSe₂; (b) (001) reflection peak of XRD pattern for selected SnSe₂ and Li_{0.2}SnSe₂ samples; (c) Schematic structural model for organic cointercalated Li_{*x*}(THF)_{*y*}SnSe₂; (d) (001) reflection peak of XRD pattern for SnSe₂, Li_{0.2}(THF)_{*y*}SnSe₂, and Li_{0.2}(PC)_{*y*}SnSe₂ samples. The Li content in the Li_{0.2}SnSe₂, Li_{0.2}(THF)_{*y*}SnSe₂, and Li_{0.2}(PC)_{*y*}SnSe₂ samples was determined through inductively coupled plasma mass spectroscopy (ICP-MS).

As seen in Figure 1a-b, in the *n*-BuLi/hexane process from method (i), Li atoms are solely intercalated into the interlayer space. Due to the small size and relatively small doping levels of Li ions, we observe only a small lattice shift (~ 0.1°) with only Li intercalation. Such shift indicates *c* lattice parameters expands very slightly from 6.137 Å in parent SnSe₂ to 6.180 Å in the intercalated Li_{0.2}SnSe₂.

On the other hand, as seen in Figure 1c-d, the lattice parameter *c* expands dramatically with the presence of cointercalated organic THF and PC molecules synthesized following processes (ii) and (iii). The basal spacing of the compound has been increased from 6.137 Å from SnSe₂, to 10.341 Å in the Li_{0.2}(THF)_{*y*}SnSe₂ compound. There is some

small amount ($< 10\%$) of SnSe_2 that remains unreacted during the intercalation which does not reduce with longer intercalation times nor slightly elevated reaction temperatures (e.g. using a hot plate). For the $\text{Li}_x(\text{PC})_y\text{SnSe}_2$ sample, the basal spacing is further increased to 12.081 \AA due to the stronger cation-dipole interaction of PC comparing to THF (dipole moment is 4.94 D for PC, and 1.63 D for THF, $1\text{D} = 3.3356 \times 10^{-30} \text{ Cm}$) [53]. However, this cointercalation process is quite inefficient, with large amount of Li_xSnSe_2 from $n\text{-BuLi}$ /hexane left, shown in Figure 1d. The peak at 11.4° , corresponding to a 7.79 \AA basal spacing, suggests that a possible different intercalation stage, i.e phase separation, exists in the particular sample.

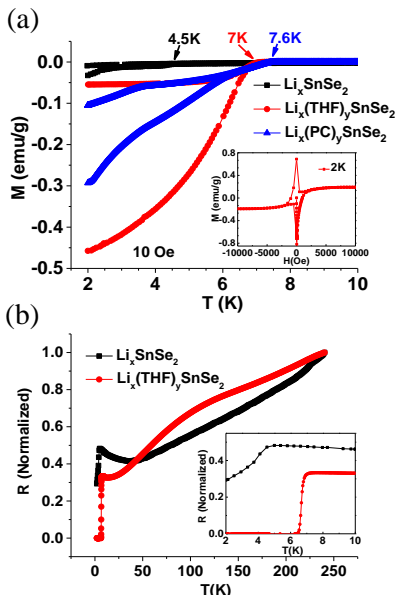


FIG. 2. (a) Magnetic susceptibility data for of Li and cointercalated SnSe_2 samples, where all three samples show diamagnetic signals; (b) Normalized temperature dependent resistivity data. The inset of (a) is the MH loop of $\text{Li}_{0.2}(\text{THF})_y\text{SnSe}_2$ at 2 K, and inset of (b) is the enlarged resistivity data highlighting superconducting transition at low temperature from 2 - 10 K.

The cointercalation of organic THF and PC molecules is further evidenced by Thermogravimetric Analysis (TGA) measurements (see supplemental materials). $\text{Li}_{0.2}(\text{THF})_y\text{SnSe}_2$ starts to decompose at $\sim 50^\circ\text{C}$ through the loss of THF and $\text{Li}_{0.2}(\text{PC})_y\text{SnSe}_2$ begins decomposition at 80°C ; in both cases these reactions are endothermic in nature. However, given the presence of unreacted SnSe_2 , Li_xSnSe_2 , and the additional issue of possible phase separation, it is rather difficult to determine the precise amount of organic species in the cointercalated samples.

The dc magnetization of intercalated $\text{Li}_{0.2}\text{SnSe}_2$, $\text{Li}_{0.2}(\text{THF})_y\text{SnSe}_2$, and $\text{Li}_{0.2}(\text{PC})_y\text{SnSe}_2$ are shown in the Figure 2a. We can see a clear enhancement of the transition temperature as the basal spacing is increased after intercalation/cointercalation processes. In the $\text{Li}_{0.2}\text{SnSe}_2$ sample, a small diamagnetic shift emerges from $\sim 4 \text{ K}$ under zero field cool (ZFC) with a very small shielding fraction, suggesting the

presence of non-bulk superconductivity in the sample. In contrast, for $\text{Li}_{0.2}(\text{THF})_y\text{SnSe}_2$, a much large diamagnetic signal from 7 K is observed. In addition, the M-H curve, shown in Figure 2a, suggests that type-II superconductivity is present in this sample. As previously noted, the $\text{Li}_{0.2}(\text{PC})_y\text{SnSe}_2$ sample exhibits a further increased basal spacing. Further buttressing the relationship between basal spacing and T_c , we note a concomitant increase in the superconducting transition temperature in $\text{Li}_{0.2}(\text{PC})_y\text{SnSe}_2$, with a further enhancement to 7.6 K . However, in the $\text{Li}_{0.2}(\text{PC})_y\text{SnSe}_2$ sample, both zero field cooling (ZFC) and field cooling (FC) data show an additional field expulsion below 4 K , which could be caused by Li_xSnSe_2 or phase separation caused by another stage of intercalation.

The superconducting behavior in these samples can be further verified by the resistivity measurement shown in the Figure 2b. The resistivity measurements confirm the superconducting temperatures of 4.5 K and 7 K for $\text{Li}_{0.2}\text{SnSe}_2$ and $\text{Li}_{0.2}(\text{THF})_y\text{SnSe}_2$, respectively, consistent with the magnetic measurements. For $\text{Li}_{0.2}\text{SnSe}_2$, only a 50% resistivity drop is observed, supporting the hypothesis of non-bulk superconductivity in the sample. For $\text{Li}_{0.2}(\text{THF})_y\text{SnSe}_2$, the superconducting transition is quite sharp and the resistivity reaches to zero at 6.4 K with a transition width $< 0.6 \text{ K}$. The $\text{Li}_{0.2}(\text{PC})_y\text{SnSe}_2$ sample is very difficult to compress as a small pellet after intercalation. Therefore, no resistivity measurement is attempted for this sample. It is worthwhile to mention that a clear hump in the $\rho(T)$ curve is present at $\sim 100 \text{ K}$ for $\text{Li}_{0.2}(\text{THF})_y\text{SnSe}_2$, reminiscent to previous investigations of metallocene-intercalated SnSe_2 [44,54]. Similar as the other TMDs such as NbSe_2 , this hump might associate with the charge density wave (CDW) transition, as a result of two dimensional Fermi surface nesting. Because the Li content, i.e. charge carrier changes, is the same for the $\text{Li}_{0.2}\text{SnSe}_2$ and $\text{Li}_{0.2}(\text{THF})_y\text{SnSe}_2$ samples, this suggests that CDW, rather than charge carrier density, may play an important role for the occurrence of bulk superconductivity, and enhanced T_c comparing with the gating technique.

Due to the presence of non-bulk superconductivity in Li_xSnSe_2 and the second transition noted in the $\text{Li}_x(\text{PC})_y\text{SnSe}_2$ samples, we focused our studies of the carrier change effects on the $\text{Li}_x(\text{THF})_y\text{SnSe}_2$ sample. The amount of lithium uptake by SnSe_2 could be controlled by changing the amount of Naph.-Li used. Indeed, the ICP-MS measurement has shown we obtained different $x=0.01 - 0.30$ samples through this method. On the other hand, no significant basal spacing increase is observed from the XRD patterns, indicating the amount of THF uptake is nearly the same for all these $\text{Li}_x(\text{THF})_y\text{SnSe}_2$ samples with different Li content since the THF is abundant as the solvent. We show the temperature dependent resistivity data on these samples in Figure 3a. SnSe_2 is semiconducting with an indirect band gap 1.07 eV [40]. As the Li doping increases, the progressive suppression of the insulating behavior can be clearly seen. A slight resistivity drop is observed for $x = 0.03$ even though the overall bulk material is still insulating, suggesting the emergence of superconductivity at this composition. Upon further Li doping, the magnitude of the superconducting

diamagnetic response increases and the $\rho(T)$ data show true zero-resistivity behavior. However, both resistivity and magnetic measurements show that the T_c is *more or less independent* of the Li doping level x for $x > 0.03$ throughout of the region, in contrast to the conventional superconductivity. Taking the conventional cross point of the two slopes as the superconducting transition temperature T_c from the resistivity and ZFC magnetic data, our summarized basal spacing, and doping level x dependent T_c is shown in the Figure 4.

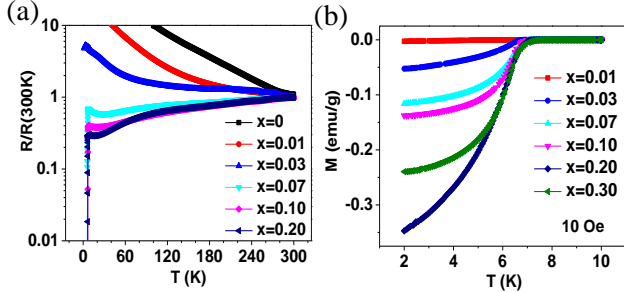


FIG. 3. (a) Normalized resistivity data of $\text{Li}_x(\text{THF})_y\text{SnSe}_2$ with different Li concentrations from $0 \leq x \leq 0.2$; (b) Zero field cooled (ZFC) magnetization data for different $\text{Li}_x(\text{THF})_y\text{SnSe}_2$ under 10 Oe field. The Li content is determined through the ICP-MS method.

We observed a monotonic increase in T_c with basal spacing, in the Figure 4a. However, this trend does not completely rule out the possibility of a dome-like T_c vs basal spacing behavior upon further intercalation, as seen in the intercalated ZrNCl system [55]. The second trend is that T_c is independent of Li concentration for $x > 0.03$, shown in the Figure 4b. This behavior is very similar to the intercalated $\text{ZrNCl}/\text{HfNCl}$ system where it was attributed to the x -independent $N(0)$ characteristics of a nearly-free electron two dimensional system [56-59]. Charge fluctuations associated with the CDW transition might therefore play an important role to induce superconductivity in these intercalated systems.

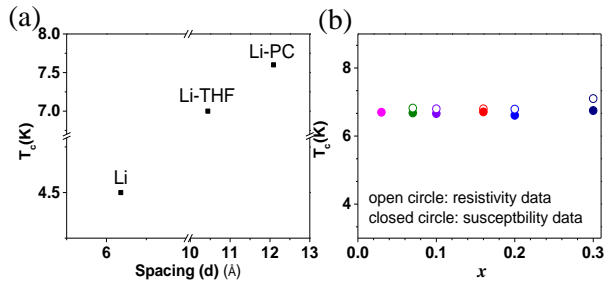


FIG.4. (a) Superconducting T_c values with respect of the basal spacing distances; (b) T_c values plotted as a function of doping level in $\text{Li}_x(\text{THF})_y\text{SnSe}_2$ showing x independent T_c .

In Figure 5 we show the field dependent resistivity data of $\text{Li}_{0.2}(\text{THF})_y\text{SnSe}_2$. The noise near room temperature is likely associated with the condensation of moisture in the samples, since the sample is very air sensitive. The small upturn in $\rho(T)$ clearly visible prior to the superconducting transition can be ascribed to the Anderson localization effect caused by inhomogeneity and disorder in the cointercalated samples [60].

Upon the application of the magnetic field, the superconducting transition is both suppressed and broadened, as expected. However, when we plot the upper critical field H_{c2} as a function of temperature (Figure 5) we note a very steep increase in the value of H_{c2} with temperature. Using a simple linear extrapolation, the zero-temperature upper critical field, $\mu_0 H_{c2}(0)$, is estimated to be 9 T. In contrast, if we apply the Werhmer-Helfand-Hohenberge (WHH) model where only the orbital effect is taken into account, the estimated $\mu_0 H_{c2}(0)$ is about 2.3 T. Such upper critical field behavior indicates increased anisotropy and likely multiband superconductivity nature in this system.

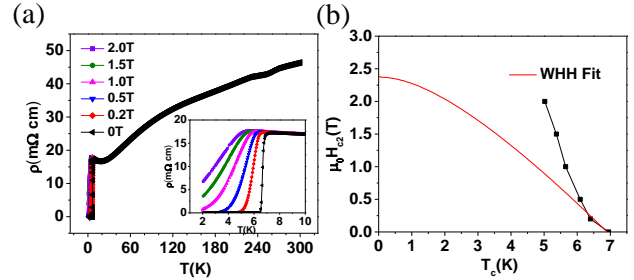


FIG. 5. (a) Field dependence of resistivity data and enlarged view of low temperature region in insert for $\text{Li}_{0.2}(\text{THF})_y\text{SnSe}_2$ sample; (b) Upper critical field determined from resistivity data. The red curve is fitting curve from WHH model.

Specific heat data were performed to get further insight of the superconductivity. Unfortunately we did not observe any clear superconducting transition at 7 K for zero field data. By subtracting the data of zero field to that of high magnetic field, we can only see a very tiny specific jump. We compared the specific data of parent compound and the superconducting sample, shown in the Fig. 5. By Debye fitting of the data using $C = \gamma_N T + \beta T^3$, we can get $\gamma_N \sim 0$ and $\beta = 1.016 \text{ mJ/mol K}^4$ and $\gamma_N = 0.654 \text{ mJ/mol K}^2$ and $\beta = 1.228 \text{ mJ/mol K}^4$, which corresponds to the electronic Sommerfeld coefficient and Debye temperature, for parent and superconducting samples respectively. The Debye temperature can be derived from the β value through the relationship $\theta_D = (12\pi^4 k_B N_A Z / 5\beta)^{1/3}$, where N_A is the Avogadro constant, and Z is the number of atoms in the molecule. The calculated Debye temperature is 180 K and 166 K for parent and superconducting compounds respectively.

As the Sommerfeld coefficient corresponding to the density of states at Fermi level, with $\gamma_N \sim 0$ corresponding to the insulating properties of the parent compound. Once we introduce electrons through chemical intercalation, a small value of Sommerfeld coefficient $\gamma_N = 0.654 \text{ mJ/mol K}^2$ will be introduced. If we take this value to $\Delta C / \gamma_N T_c = 1.43$ for the BCS theory, the specific jump $\Delta C / T$ at the transition temperature is 0.94 mJ/mol K^2 , only 2% of the specific heat value at T_c , which could be a possible reason we did not observe the specific jump. Similar small Sommerfeld coefficient is also observed in the Li_xZrNCl system. If we compare γ_N and T_c for Li_xZrNCl and $\text{Li}_x(\text{THF})_y\text{SnSe}_2$, with $\gamma_N \sim 1 \text{ mJ/mol K}^2$ and $T_c \sim 12 \text{ K}$ for Li_xZrNCl and $\gamma_N \sim 0.65 \text{ mJ/mol K}^2$ and $T_c = 6.9 \text{ K}$ for $\text{Li}_x(\text{THF})_y\text{SnSe}_2$, almost the same ratio between γ_N and T_c is obtained. The close relationship between Li_xZrNCl and

$\text{Li}_x(\text{THF})_y\text{SnSe}_2$ may indicate unconventional superconductivity of the co-intercalated SnSe_2 [61,62].

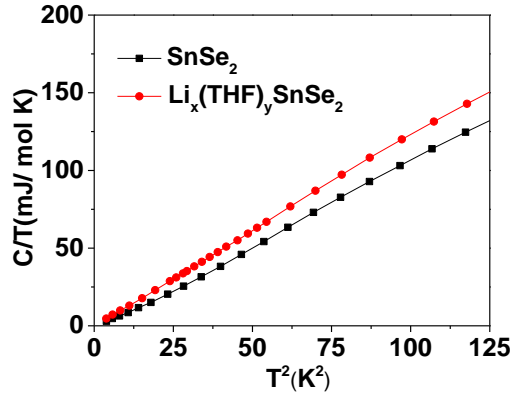


FIG. 6. Heat capacity data of parent and cointercalated SnSe_2 samples.

IV. CONCLUSIONS

In summary, chemical intercalation through both Li doping and the incorporation of organic THF and PC molecules has

been carried out in 1T two dimensional SnSe_2 phase. We induced superconductivity with values of up to 7.6 K where the transition temperature T_c is found to be significantly enhanced by incorporation of polar organic molecules during the intercalation process. Detailed studies suggests the T_c is almost independent from carrier concentration, but rather correlated with the basal spacing distances. Our results suggest that the charge fluctuation mechanism may play an important role for the unconventional superconductivity present in this system.

ACKNOWLEDGMENT

This work at University of Texas at Dallas is supported by US Air Force Office of Scientific Research Grant No. FA9550-15-1-0236, FA9550-19-1-0037, and the startup funds from University of Texas at Dallas. The work at AFRL was also supported by an AFOSR grant (LRIR 18RQCOR100) and a grant from the National Research Council. SK and MJK acknowledges the support from Louis Beecherl, Jr. endowed funds.

-
- [1] K. F. Mak, C. Lee, J. Hone, J. Shan, and T. F. Heinz, *Phys. Rev. Lett.* **105**, 136805 (2010).
 - [2] A. Splendiani, L. Sun, Y. Zhang, T. Li, J. Kim, C. Chim, G. Galli, and F. Wang, *Nano Lett.* **10**, 1271–1275 (2010).
 - [3] D. H. Keum, S. Cho, J. H. Kim, D. Choe, H. Sung, M. Kan, H. Kang, J. Hwang, S. W. Kim, H. Yang, K. J. Chang, and Y. H. Lee, *Nat. Phys.* **11**, 482–486 (2015).
 - [4] S. Wu, V. Fatemi, Q. D. Gibson, K. Watanabe, T. Taniguchi, R. J. Cava, and P. Jarillo-Herrero, *Science* **359**, 76-79 (2018).
 - [5] Z. Fei, T. Palomaki, S. Wu, W. Zhao, X. Cai, B. Sun, P. Nguyen, J. Finney, X. Xu, and D. H. Cobden, *Nat. Phys.* **13**, 677–682 (2017).
 - [6] S. Tang, C. Zhang, D. Wong, Z. Pedramrazi, H. Tsai, C. Jia, B. Moritz, M. Claassen, H. Ryu, S. Kahn, J. Jiang, H. Yan, M. Hashimoto, D. Lu, R. G. Moore, C. Hwang, C. Hwang, Z. Hussain, Y. Chen, M. M. Ugeda, Z. Liu, X. Xie, T. P. Devereaux, M. F. Crommie, S. Mo, and Z. Shen, *Nat. Phys.* **13**, 683–687 (2017).
 - [7] C. Wang, Y. Zhang, J. Huang, S. Nie, G. Liu, A. Liang, Y. Zhang, B. Shen, J. Liu, C. Hu, Y. Ding, D. Liu, Y. Hu, S. He, L. Zhao, L. Yu, J. Hu, J. Wei, Z. Mao, Y. Shi, X. Jia F., Zhang, S. Zhang, F. Yang, Z. Wang, Q. Peng, H. Weng, X. Dai, Z. Fang, Z. Xu, C. Chen, and X. J. Zhou, *Phys. Rev. B* **94**, 241119(R) (2016).
 - [8] Z. Wang, D. Gresch, A. A. Soluyanov, X. Xie, S. Kushwaha, X. Dai, Troyer, M. R. J. Cava, and B. A. Bernevig, *Phys. Rev. Lett.* **117**, 056805 (2016).
 - [9] G. Wang, A. Chernikov, M. M. Glazov, T. F. Heinz, X. Marie, T. Amand, and B. Urbaszek, *Rev. Mod. Phys.* **90**, 021001 (2018).
 - [10] F. Zhang, J. Jung, G. A. Fiete, Q. Niu, and A. H. MacDonald, *Phys. Rev. Lett.* **106**, 156801 (2011).
 - [11] I. Martin, Y. M. Blanter, and A. F. Morpurgo, *Phys. Rev. Lett.* **100**, 036804 (2008).
 - [12] A. Vaezi, Y. Liang, D. H. Ngai, L. Yang, and E.-A. Kim, *Phys. Rev. X* **3**, 021018 (2013).
 - [13] J. R. Schaibley, H. Yu, G. Clark, P. Rivera, J. S. Ross, K. L. Seyler, W. Yao, and X. Xu, *Nat. Rev. Mater.* **1**, 16055 (2016).
 - [14] D. Shin, H. Hübener, U. D. Giovannini, H. Jin, A. Rubio, and N. Park, *Nat. Commun.* **9**, 638 (2018).
 - [15] M. Chhowalla, D. Jena, and H. Zhang, *Nat. Rev. Mater.* **1**, 16052 (2016).
 - [16] K. F. Mak, and J. Shan, *Nat. Photonics* **10**, 216–226 (2016).
 - [17] J. Cheng, C. Wang, X. Zou, and L. Liao, *Adv. Optical Mater.* **7**, 1800441 (2019).
 - [18] A. F. Morpurgo, *Nat. Phys.* **9**, 532–533 (2013).
 - [19] F. A. Levy, *Intercalated Layered Materials* (Dordrecht, 1979).

- [20] R. H. Friend, and A. D. Yoffe, *Adv. Phys.* **36**, 1-94 (1987).
- [21] X. Li, and Y. Li, *J. Phys. Chem. B* **108**, 13893-13900 (2004).
- [22] A. Ambrosi, Z. Sofer, and M. Pumera, *Small* **11**, 605 (2015).
- [23] K. Takada, H. Sakurai, E. Takayama-Muromachi, F. Izumi, R. A. Dilanian, and T. Sasaki, *Nature* **422**, 53-55 (2003).
- [24] S. Yamanaka, K. Hotehama, and H. Kawaji, *Nature* **392**, 580-582 (1998).
- [25] N. Emery, C. Hérold, J.-F. Maréché, and P. Lagrange, *Sci. Technol. Adv. Mater.* **9**, 044102 (2008).
- [26] R. A. Klemm, *Physica C* **514**, 86–94 (2015).
- [27] R. Zhang, I.-L. Tsai, J. Chapman, E. Khestanova, J. Waters, and I. V. Grigorieva, *Nano Lett.* **16**, 629–636 (2016).
- [28] E. Morosan, H. W. Zandbergen, B. S. Dennis, J. W. G. Bos, Y. Onose, T. Klimczuk, A. P. Ramirez, N. P. Ong, and R. J. Cava, *Nat. Phys.* **2**, 544–550 (2006).
- [29] X. Miao, S. Nishiyama, L. Zheng, H. Goto, R. Eguchi, H. Ota, T. Kambe, K. Terashima, T. Yokoya, H. T. Nguyen, T. Kagayama, N. Hirao, Y. Ohishi, H. Ishii, Y. F. Liao, and Y. Kubozono, *Sci. Rep.* **6**, 29292 (2016).
- [30] K. Sato, T. Noji, T. Hatakeda, T. Kawamata, M. Kato, and Y. Koike, *J. Phys. Soc. Jpn.* **86**, 104701 (2017).
- [31] K. Sato, T. Noji, T. Hatakeda, T. Kawamata, M. Kato, and Y. Koike, arXiv 1805.11977.
- [32] Y. Saito, Y. Kasahara, J. Ye, Y. Iwasa, and T. Nojima, *Science*, **350**, 409-413 (2015).
- [33] J. T. Ye, Y. J. Zhang, R. Akashi, M. S. Bahramy, R. Arita, and Y. Iwasa, *Science*, **338**, 1193-1196 (2012).
- [34] D. Costanzo, S. Jo, H. Berger, and A. F. Morpurgo, *Nat. Nanotech.* **11**, 339–344 (2016).
- [35] J. T. Ye, S. Inoue, K. Kobayashi, Y. Kasahara, H. T. Yuan, H. Shimotani, and Y. Iwasa, *Nat. Mater.* **9**, 125–128 (2010).
- [36] J. M. Lu, O. Zheliuk, I. Leermakers, N. F. Q. Yuan, U. Zeitler, K. T. Law, and J. T. Ye, *Science* **350**, 1353-1357 (2015).
- [37] E. Sajadi, T. Palomaki, Z. Fei, W. Zhao, P. Bement, C. Olsen, S. Luescher, X. Xu, J. A. Folk, and D. H. Cobden, *Science* **362**, 922-925 (2018).
- [38] V. Fatemi, S. Wu, Y. Cao, L. Bretheau, Q. D. Gibson, K. Watanabe, T. Taniguchi, R. J. Cava, and P. Jarillo-Herrero, *Science* **362**, 926-929 (2018).
- [39] X. He, and H. Shen, *Phys. B.* **407**, 1146–1152 (2012).
- [40] J. M. Gonzalez, and I. I. Oleynik, *Phys. Rev. B.* **94**, 125443 (2016).
- [41] G. Busch, C. Froehlich, and F. Hulliger, *Helv. Phys. Acta.* **34**, 359-368 (1961).
- [42] D. O'Hare, J. S. O. Evans, P. J. Wiseman, and K. Prout, *Angew. Chem. Int. Ed.* **30**, 1156-1158 (1991).
- [43] C. A. Formstone, E. T. FitzGerald, D. O'Hare, P. A. Cox, M. Kurmoo, J. W. Hodby, D. Lillicrap, and M. Goss-Custard, *Soc. Chem. Commun.* **0**, 501-503 (1990).
- [44] D. O'Hare, H. Wong, S. Hazell, and J. W. Hodby, *Adv. Mater.* **4**, 658 (1992).
- [45] J. Zeng, E. Liu, Y. Fu, Z. Chen, C. Pan, C. Wang, M. Wang, Y. Wang, K. Xu, S. Cai, X. Yan, Y. Wang, X. Liu, P. Wang, S. Liang, Y. Cui, H. Y. Hwang, H. Yuan, and F. Miao, *Nano. Lett.* **18**, 1410–1415 (2018).
- [46] Y. Mao, H. Shan J., Wu, Z. Li, C. Wu, X. Zhai, A. Zhao, and B. Wang, arXiv:1712.10100.
- [47] Y. Zhang, J. Fan, W. Wang, D. Zhang, L. Wang, W. Li, K. He, C. Song, X. Ma, and Q. Xue, arXiv:1802.08434v1.
- [48] X. Yu, J. Zhu, Y. Zhang, J. Weng, H. Hua, and S. Dai, *Chem. Commun.* **48**, 3324-3326 (2012).
- [49] J. Choi, J. Jin, I. Jung, J. M. Kim, H. J. Kim, and S. U. Son, *Chem. Commun.* **47**, 5241-5243 (2011).
- [50] F. Zhang, C. Xia, J. Zhu, B. Ahmed, H. Liang, D. B. Velusamy, U. Schwingenschlögl, and H. A. Alshareef, *Adv. Energy Mater.* **6**, 1601188 (2016).
- [51] Y. Su, M. A. Ebrish, E. J. Olson, and S. J. Koester, *Appl. Phys. Lett.* **103**, 263104 (2013).
- [52] E. P. Mukhokosi, S. B. Krupanidhi, and K. K. Nanda, *Sci. Rep.* **7**, 15215 (2017).
- [53] R. C. Weast, *CRC Handbook of Chemistry and Physics 58th ed* (1977).
- [54] Z. Li, Y. Zhao, K. Mu, H. Shan, Y. Guo, J. Wu, Y. Su, Q. Wu, Z. Sun, A. Zhao, X. Cui, C. Wu, and Y. Xie, *J. Am. Chem. Soc.* **139**, 16398–16404 (2017).
- [55] K. Hotehama, T. Koiwasaki, K. Umemoto, S. Yamanaka, and H. Tou, *J. Phys. Soc. Jpn.* **79**, 014707 (2010).
- [56] I. Hase, and Y. Nishihara, *Phys. Rev. B.* **60**, 1573 (1999).
- [57] R. Weht, A. Filippetti, and W. E. Pickett, *Europhys. Lett.* **48**, 320 (1999).
- [58] C. Felser, and R. Seshadri, *J. Mater. Chem.* **9**, 459 (1999).
- [59] H. Sugimoto, and T. Oguchi, *J. Phys. Soc. Jpn.* **73**, 2771 (2004).
- [60] T. Taguchi, A. Kitora, and Y. Iwasa, *Phys. Rev. Lett.* **97**, 107001 (2006).
- [61] T. Taguchi, M. Hisakabe, and Y. Iwasa, *Phys. Rev. Lett.* **94**, 217002 (2005).
- [62] Y. Kasahara, T. Kishiume, T. Takano, K. Kobayashi, E. Matsuoka, H. Onodera, K. Kuroki, Y. Taguchi, and Y. Iwasa, *Phys. Rev. Lett.* **103**, 077004 (2009).